

On the Friction and Wear Behaviors of PTFE Based Composites Filled with MoS₂ and/or Bronze Particles

M. Trabelsi¹ · M. Kharrat¹ · M. Dammak¹

Received: 12 September 2014 / Accepted: 18 August 2015 / Published online: 15 October 2015
© The Indian Institute of Metals - IIM 2015

Abstract This paper accounts for the commercial polytetrafluoroethylene (PTFE) based composites, filled with molybdenum disulfide (MoS₂) and/or bronze particles. Fire loss technique followed by atomic absorption analyses is used here to identify the weight fractions of their constituents. The mechanical properties of the composites are characterized using tensile and hardness tests. The results show that the ultimate strength decreases with the addition of MoS₂. Friction and wear behaviors of the different types of PTFE composites sliding against 100Cr6 steel ball are investigated under dry conditions using reciprocating linear tribometer. Experimental results show that the addition of MoS₂ in the PTFE–bronze composite reduces the wear of this composite. Its friction coefficient undergoes a sharp increase at the end of the test. Scanning electron microscopy examination shows some micro cracks and flake pieces on its worn surface and an abrasive wear mechanism is identified on the steel counter face using an optical microscope.

Keywords PTFE · Composite · Bronze · MoS₂ · Friction · Wear

1 Introduction

In service, mechanical seals and guide way or slide way surfaces are subjected to friction and wear against steel counter faces. A good understanding of this phenomenon is

required to improve the energy safeguard and the durability of these elements. Currently, thermoplastics, thermosets and composites are being used as sliding surfaces. Among the polymers which are extensively used as mechanical seals, slide ways or guide ways surfaces, polytetrafluoroethylene (PTFE) polymer is most significant due to its low friction coefficient, self-lubricant material, as well as good resistance to solvents [1–5]. For this thermoplastic polymer, the low friction coefficient results from the formation of a thin transfer film on the sliding counter face [6, 7]. Nevertheless, the formation and alteration of this transfer film occurs with a high frequency, causing a poor wear resistance for the PTFE, which poses a serious problem for the use of this polymer in tribological applications [2]. The most effective way of increasing the wear resistance of PTFE is by the incorporation of small size fillers such as bronze [1, 2, 4, 6–8], carbon fibers [9], glass fibers [7, 10–12], ZnO [13], alumina [3], SiO₂ [14]. Jisheng and Gawne [1] investigated the friction and wear properties of a bronze-filled PTFE composite by sliding against cast iron. They noted that PTFE–bronze composite shows a superior wear resistance to either of its constituents in their pure states. According to their research work, the amount of bronze particles at the surface increased substantially with the progress of sliding. The PTFE is preferentially removed from the surface and the bronze particles are pressed deeper into the matrix and resulting in an increased area fraction of the bronze at the contact surface. The authors concluded that the reduction of the wear rate was the result of the effect of the bronze particles which provided a blocking action on the slip of the PTFE individual crystalline lamellae or bands. Wang and Yan [6] prepared the transfer films of PTFE/bronze composite by sliding against a steel surface under a designed condition. The authors investigated the shape, thickness and tribological

✉ M. Kharrat
mohamed.kharrat@ipeis.rnu.tn

¹ Laboratory of Electromechanical Systems, National Engineering School of Sfax, Soukra Road, Km 3.5, B.P. 1173, 3038 Sfax, Tunisia

behavior of the obtained transfer films just as what had been done on common films or coatings. They found that the tribological properties of the corresponding transfer films were improved by a higher bronze content in the composite. Also, the friction coefficient was reduced and wear life of this film was prolonged. Tanaka and Kawakami [7] studied the wear reducing actions of various types of fillers in PTFE based composites. They found that the fibers and not small particles, improved the wear resistance more effectively than MoS₂, graphite powders or even very small hard particles. The improved wear attributed to the effect of the fillers which supported the load and obstructed the fragmentation of the PTFE matrix. Moreover, the authors concluded that the improvement of the wear resistance of the PTFE-based composites was dependent on the material, shape, and size of the filler. Other authors [3, 15, 16], reported that the addition of the hard filler particles could improve the wear resistance and rigidity of matrix but it could also cause an increase of the dry sliding friction coefficient and abrasion of the counter face.

In this paper, the attempt was made to compare and predict the friction and wear performance of PTFE based composites filled with MoS₂ and/or bronze particles using a reciprocating tribometer. For each of the considered composites, the evolution of the friction coefficient, the wear rate and wear process with respect to the number of sliding cycles were analyzed.

2 Experimental Details

2.1 PTFE-Based Composites

Pure commercial PTFE and three PTFE composite materials used for guide rings were considered in this study. They were supplied as strips with a cross-section of 25 × 3 mm². The filler particles added to the PTFE matrix were bronze and bronze + MoS₂. For each composite material, the weight fractions of the constituents were identified using fire loss technique followed by atomic absorption analyses.

For fire loss technique, a programmable, electrical oven was employed to heat an amount of each sample of the

composite materials until 530 °C at 20 °C/min. This heating cycle allowed the polymer to burn completely. The remaining weight fraction was the filler content plus a fine powder of fluoride products. After that, a good shake and heating dissolved the residual product in a concentrated mixture of hydrochloric acid and nitric acid in the proportions of 2/3 and 1/3 respectively. This process continues until the liquid totally evaporates and minerals precipitate themselves. Then with a good shake, the minerals were dissolved in distillate water. For the atomic absorption analysis, a sample of 150 ml of the obtained solution was used to determine the concentration of the different elements as copper, zinc, molybdenum and lead. The characteristics of the fillers were determined by optical microscope. The results are listed in Table 1.

2.2 Failure Analysis

LEICA DMILM optical microscope (OM) (Leica, Germany) was used to observe the microstructural features of specimens before and after the wear test, respectively. Also, the OM was utilized to observe the surface of the steel counter faces for different test durations. Moreover, scanning electron microscopy (SEM) has been used to analyze the worn surfaces of composite specimens and to study the possible modes of failure. Also, SEM and OM were utilized to characterize the debris of the wear testing.

2.3 Tensile Test

The mechanical properties of the pure PTFE and the PTFE composite materials were determined under tensile loading. The stress–strain curve of each specimen was obtained from a LLOYD/LR 5K testing machine (LLOYD, USA) equipped with a 5 KN load cell and 25 mm displacement extensometer. The crosshead speed for the tensile test was set at 5 mm/min. All tests were carried out at temperatures between 20 and 25 °C. Samples were cut from the supplied strips. The geometry of the samples was in accordance to the tensile testing norm AFNOR [17]. Three samples from each material were tested. Figure 1 shows the geometrical dimensions of the samples used for the tensile tests.

Table 1 PTFE based composite materials

Designation	PTFE (wt%)	Bronze (wt%)	MoS ₂ (wt%)	Characteristics of fillers
A	60	40	0	Bronze 10–30 μm size
B	55	40	<5	Bronze 10–30 μm size + small size MoS ₂
C	70	30	0	Bronze 10–30 μm size

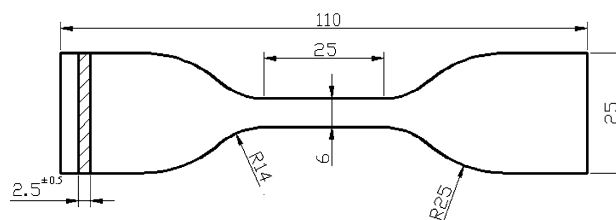


Fig. 1 Geometrical dimensions of the tensile test specimen

2.4 Hardness Test

The hardness tests were performed on a “DUROTECH model B202” (Durotech Inc, USA) hardness apparatus in accordance with the ISO 868 standards [18]. It was used to characterize the hardness of the pure PTFE and the PTFE composite materials. The specimens were 3 mm in thickness and had flat surfaces with dimensions 25 × 15 mm². A Shore D hardness test was used for hard polymeric materials. It measured the depth of penetration into the material with a conical indenter. The range of the hardness values were from 0 (for full penetration) to 100 (for no penetration). For each of the considered materials, five measurements of hardness at different positions on the specimen were performed. The mean value and the standard deviation were then calculated.

2.5 Wear Test

The friction and wear characterizations of the pure PTFE and PTFE composites were performed using a reciprocating ball-on-flat tribometer under dry conditions (Fig. 2). The specimens were cut from the supplied strips with dimensions of 20 × 25 × 3 mm³. A high chromium steel ball (100Cr6) with a diameter of 38 mm was used for the counter face. The tribometer allowed the contact between the steel ball and the composite specimen under a constant normal load of 81.3 N. The steel ball was kept stationary and a tangential cyclic motion was applied to the specimen, glued on a cubic holder, using a crank system driven by an electric motor with an electronic speed regulator. The tangential displacement amplitude and frequency were adjusted initially. A load cell located between the specimen holder and the slider of the crank system allowed measurement of the tangential force. The output of this load cell was continuously recorded using a data acquisition system. Before each test, the steel ball and the specimen surfaces were thoroughly cleaned with ethanol and then dried. The friction and wear test conditions selected for our study are given in Table 2. For each of the materials under discussion here, three tests were performed for a given test duration.

After each wear test, the cross section *S* (mm²) of the wear groove on the surface of the specimen was calculated from the established surface profile using SJ-210 Hand-held Roughness Tester (Mitutoyo, France). The volume loss *V* (mm³) of the specimen due to the wear was calculated as:

$$V = S \times d, \tag{1}$$

where *d* = 15 mm is the length of the sliding stroke and *S* is the cross-section, (mm²). The specific wear rate

K (mm³/Nm) was calculated using the following expression as explained in the ASTM standard [19]:

$$K = \frac{V}{F_n \times D} \tag{2}$$

where *F_n* is the normal load, (N), *V* the volume loss, (mm³) and *D* the sliding distance, (m).

3 Results and Discussion

3.1 Mechanical Properties

Typical stress–strain curves for pure PTFE and composites A, B and C are given in Fig. 3. The three composites experience an elasto-visco-plastic behavior and no localized necking is observed. Therefore, high values of the ultimate strain are measured from these composites. The measured values of the Young modulus, the ultimate stress and ultimate strain of the pure PTFE and the PTFE composites are given in Table 3. It can be seen that all

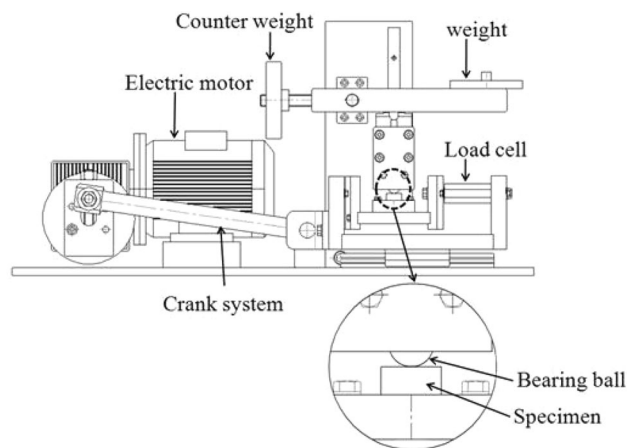


Fig. 2 Reciprocating ball-on-flat tribometer

Table 2 Friction and wear test conditions

Parameters	Experimental conditions
Normal load (N)	81.3
Displacement amplitude (mm)	±7.5
Frequency (Hz)	1
Temperature (°C)	20–25
Humidity (%)	50–60
Test duration (min)	120, 300, 420, 600
Surface roughness <i>R_a</i> (μm)	Composite A: 2.4; B: 16; C: 2.3; PTFE: 2.1

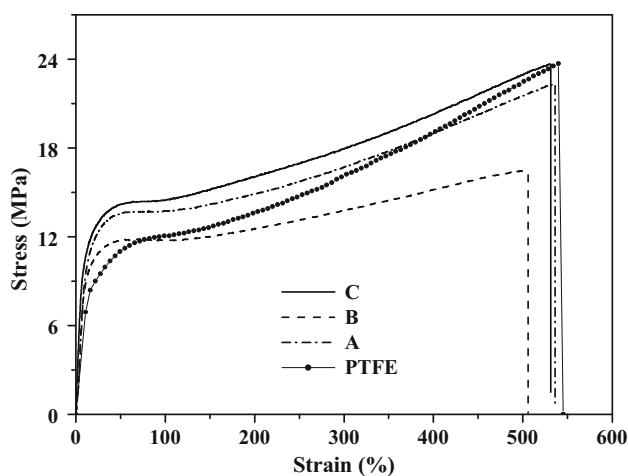


Fig. 3 Typical stress–strain curves of the pure PTFE and PTFE composites

composites have lower strength and lower ductility than the PTFE material. This is attributed to the type of the filler addition of MoS₂ and/or bronze. The composite C has a higher ultimate stress than the other two composites A and B. This is due to the lower weight fraction of filler in the composite C. Khoddamzadeh et al. [5] have reported that the ultimate strength is a function of both the content level and the type of the fillers. In fact, the consequence of the addition of fillers to the matrix is the increase in the interfaces between the matrix and the reinforcement. In these interfaces there are no strong bonds which become the places of crack initiation and the result is a lower ultimate strength accompanied with a decrease in ductility [15]. Moreover, Tanaka and Kawakami [7] reported that in the interface there is no strong adhesion between the PTFE matrix and the MoS₂ filler. Consequently, the addition of the MoS₂ to the matrix reduces the ultimate strength and the ductility of the PTFE–bronze composite.

Figure 4 shows the main values as well as standard deviations of “Shore D” hardness measured on the pure PTFE and the composites A, B and C. Composites A and B exhibit a slightly higher hardness than that of the composite C and the pure PTFE. Indeed, composites A and B contain

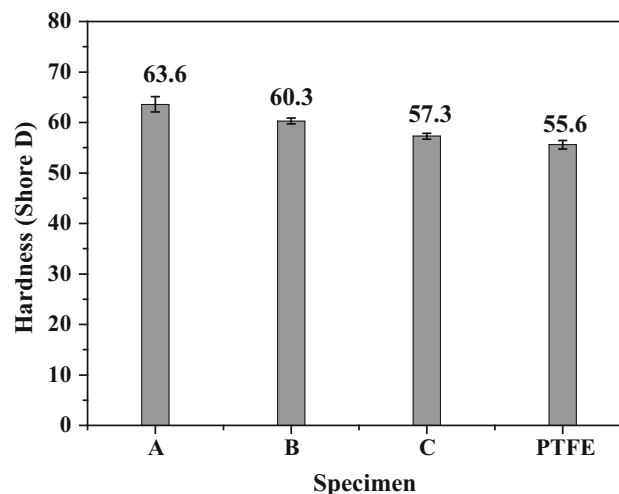


Fig. 4 The hardness of the pure PTFE and PTFE composites per unit Shore D

more fillers than composite C. As expected, the hardness of fillers affects that of the composites [5].

3.2 Friction and Wear Results

The typical evolutions of the friction coefficient with the number of cycles for the considered PTFE composites and the pure PTFE are plotted in Fig. 5. It can be seen that the friction coefficient of the pure PTFE reaches a constant value of 0.19 after 13,000 cycles. For composite A, the friction coefficient reaches a maximum value of 0.17 at the end of the running-in stage. Then, it undergoes a noticeable decrease that may be attributed to the formation of a PTFE transfer film on the steel counterface. Then, the friction coefficient experiences a smooth increase to reach a constant value of 0.15 towards the end of the test. The frictional behavior of composite C is closely similar to that of composite A. For composite C, the constant value, attained after the last stage of the test, is around 0.21. Composite B shows different frictional behavior. After the first running-in stage, its friction coefficient remains approximately constant around a value of 0.17 for the second stage. Afterward, it experiences a sharp increase near the end of the test to reach a maximum value of 0.26. It can be seen from the results of the friction tests, that the composite A has good friction behavior compared to the pure PTFE.

Typical profiles of the wear groove on the specimen’s surface for different test durations are plotted in Figs. 6, 7, 8 and 9 for the composites A, B, C and pure PTFE, respectively. From these profiles, the cross sections S (mm²) of the wear grooves are calculated. The wear loss, represented by the volume loss V (mm³), is then plotted against the number of cycles N in Fig. 10 for each of the considered composites and the pure PTFE. For each of

Table 3 Mechanical properties

	Young modulus (MPa)	Ultimate stress (MPa)	Ultimate strain (%)
Pure PTFE	495 ± 13	23.7 ± 0.4	536 ± 5
Composite A	560 ± 2	22.0 ± 0.2	531 ± 4
Composite B	582 ± 2	16.5 ± 0.2	512 ± 7
Composite C	676 ± 4	23.5 ± 0.6	521 ± 8

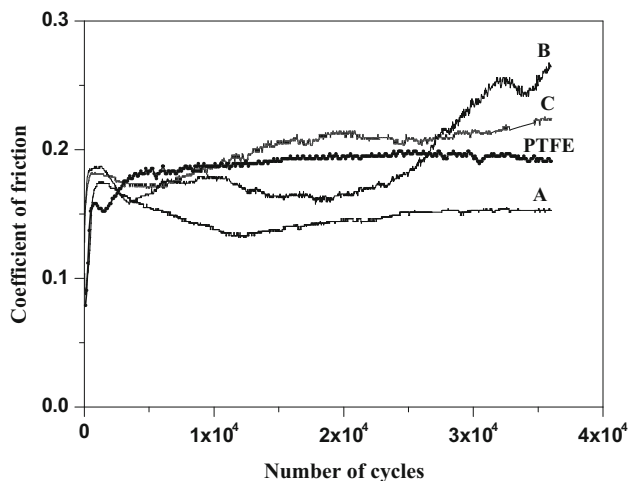


Fig. 5 Evolution of the friction coefficients with the number of cycles

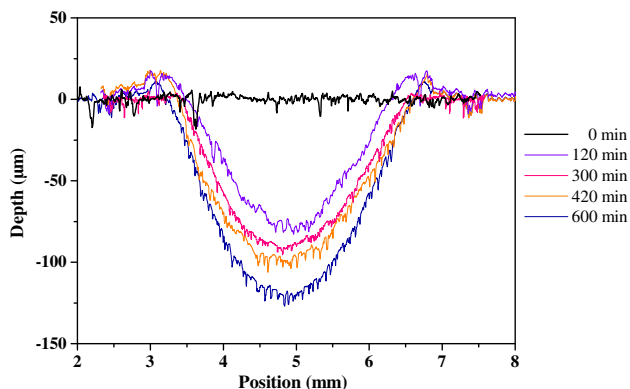


Fig. 6 Typical profiles of the wear groove: composite A

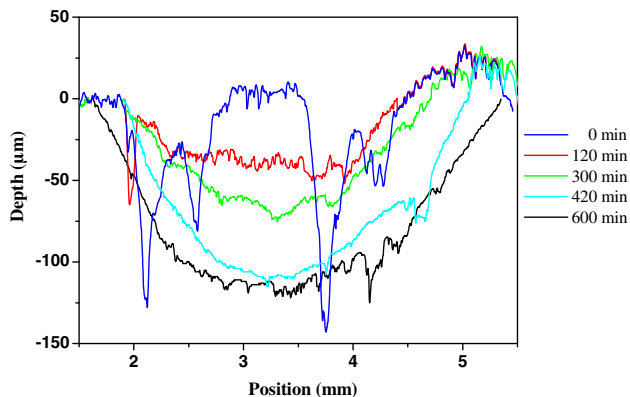


Fig. 7 Typical profiles of the wear groove: composite B

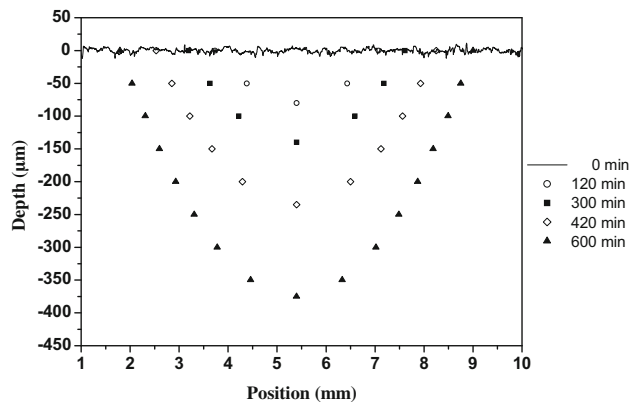


Fig. 8 Typical profiles of the wear groove: composite C

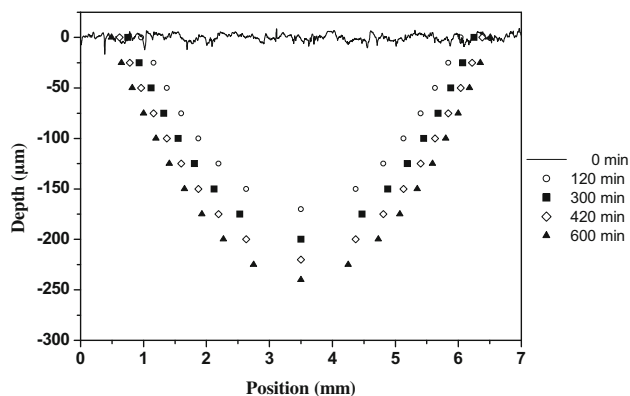


Fig. 9 Typical profiles of the wear groove: PTFE

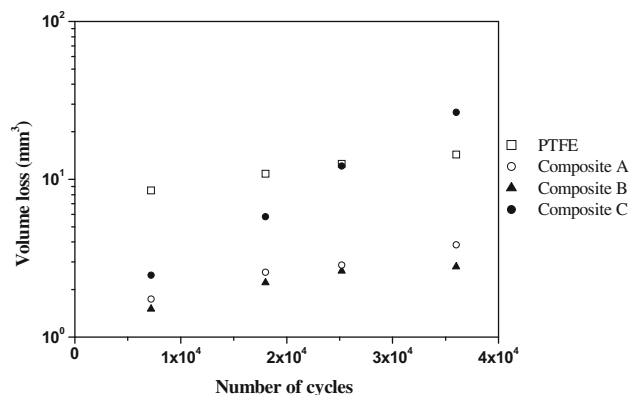


Fig. 10 Evolution of the volume losses with the number of cycles

these materials, the specific wear rate K (mm^3/Nm) is also plotted against the number of cycles in Fig. 11.

It can be seen that composite A and B exhibits the highest wear resistance compared to the composite C and the pure PTFE. It is seen that after 36,000 cycles;

Composite A is $7\times$ and composite B is $9\times$ more wear resistant than composite C. For composite A, B and the pure PTFE, the specific wear rate decreases when the number of cycles increases. Nonetheless, for composite C, the specific wear rate increases progressively and it exceeds the wear rate of the pure PTFE for 36,000 cycles.

As shown in Fig. 5, an adaptive mechanism between the composite specimen and the steel counter face is manifested in the first running-in stage for the composites A, B and C, and thus, the friction coefficient increases progressively and reaches a maximum. The friction coefficient decreases progressively in the second stage for the composites A and C, which may be attributed to the formation of a transfer film on the steel's counter face. This is confirmed by OM observations, showing wear debris on the steel counter faces after 10,000 cycles for composite A and after 2500 cycles for composite C (Fig. 12a, b). The transfer film is the result of adhesion between the contact surfaces, and some authors [20, 21], have reported that the adhesion is attributed to the chemical adhesion and mechanical entrapment. Moreover, iron is particularly reactive to PTFE and chemical bonding is considered to be

a major component of adhesion [21]. Moreover, examinations of the microstructure of specimens before and after 1500 cycles for composite A and C reveals a higher percentage of bronze on the wear track resulting from the sliding action (Fig. 13). In the final stage, the friction coefficient increases progressively and then stabilizes. The increase in the friction coefficient may be due to the destruction of the transfer film from the steel counter face, which is observed in the micrographs, showing bronze particles on the steel counter faces after 36,000 cycles for the composites A and C (Fig. 14a, b). It is well known that small particles or powder fillers are generally embedded in the PTFE matrix at the frictional surface. Besides, they are easily transferred to the counterpart surface with the matrix and are embedded in the transfer film during sliding. However, the abrasive nature of the wear debris causes the elimination of the transfer film from the steel counter face. As a result, a bed of "third body" is formed between the contacting surfaces as illustrated in the micrographs of the wear groove on the surfaces of composites A and C (Figs. 15, 16). Therefore, the stabilization of friction coefficient is due to the presence of the "third body" debris, which accommodates the sliding between the contacting surfaces during their existence in the interface.

For composite B, the friction coefficient stabilizes just after the first running-in stage. Here, a particular wear mechanism is activated as illustrated by the micrograph of Fig. 17. It is seen that the sliding track is covered by a coat which is referred to as a running film providing an effective barrier against wear. This running film cracks in both parallel and perpendicular orientations of the sliding direction. The appearance of the cracking reveals that the running film is harder and more brittle than the bulk of the material. Moreover, it is seen that after 23,500 cycles, the friction coefficient undergoes a sharp increase. From the OM analysis of the steel counter face, an abrasive wear mechanism is identified for this final stage and a series of

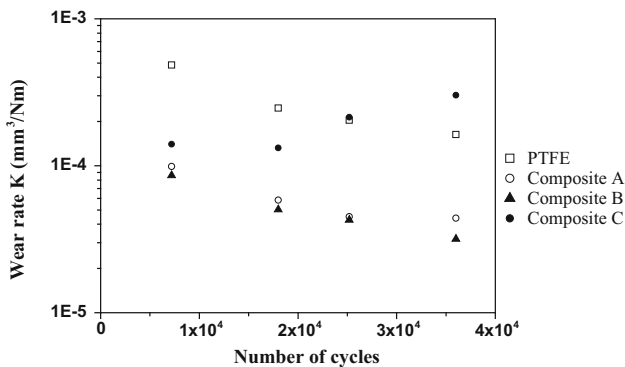


Fig. 11 Evolution of the wear rates with the number of cycles

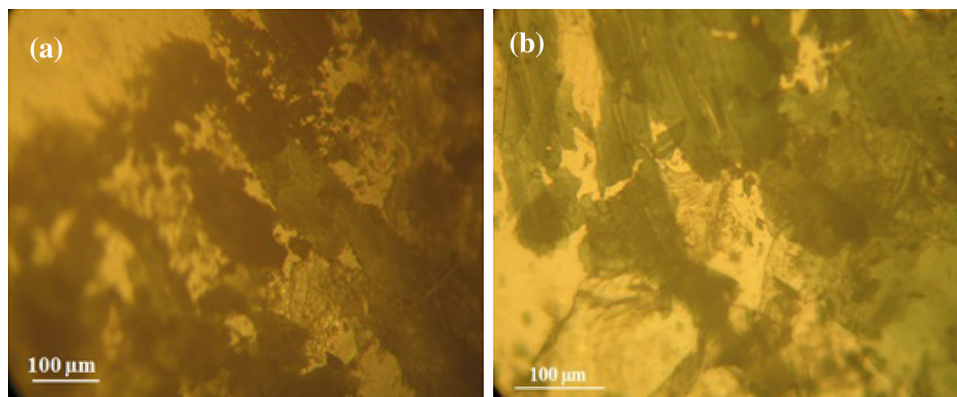


Fig. 12 Optical micrographs of the steel counterface rubbing against: **a** composite A for 10,000 cycles, and **b** composite C for 2500 cycles

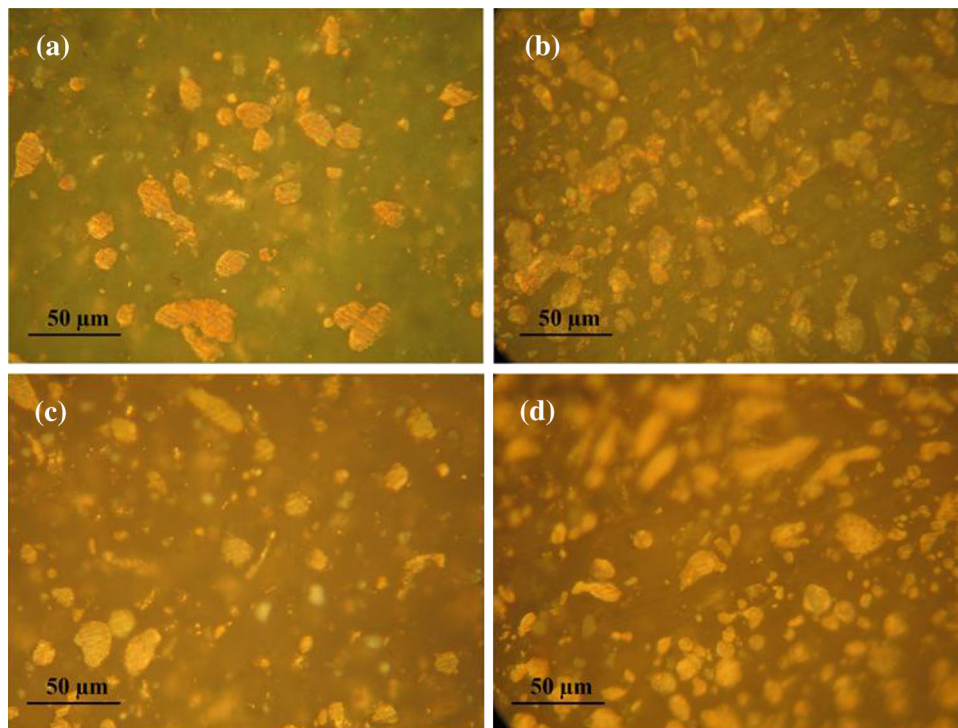


Fig. 13 Optical micrographs of the microstructure of composite A and C: **a** composite A before the wear test, **b** composite A after 1500 cycles, **c** composite C before the wear test, **d** composite C after 1500 cycles

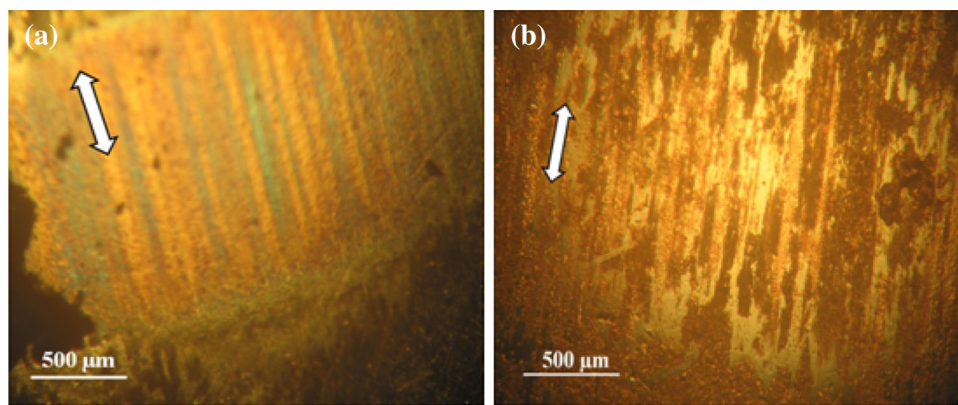


Fig. 14 Optical micrographs of the steel counterface rubbing for 36,000 cycles against: **a** composite A, and **b** composite C

grooves in parallel with the sliding direction is observed after 36,000 cycles (Fig. 18). This behavior may be attributed to the detached flake pieces from the running film which have an abrasive effect on the steel counterface. These flake pieces are composed of MoS_2 and PTFE and their high hardness may be due to the oxidation of the MoS_2 fillers achieving a layered structure of MoO_3 during sliding [22, 23]. Moreover, flake pieces cannot be easily detached from the frictional surface. This behavior can be attributed to the presence of bronze particles, which act as

effective barriers to prevent large-scale fragmentation of PTFE as illustrated in the micrograph of Fig. 19 and reported by other research studies [2, 24]. Consequently, a transfer film of PTFE is not formed on the steel counterface.

Despite its higher coefficient of friction, composite B exhibits the highest wear resistance compared to the two other composites. The MoS_2 particles along with bronze provides enhanced wear behavior. Composite A has a good wear resistance which is comparable to that of composite B

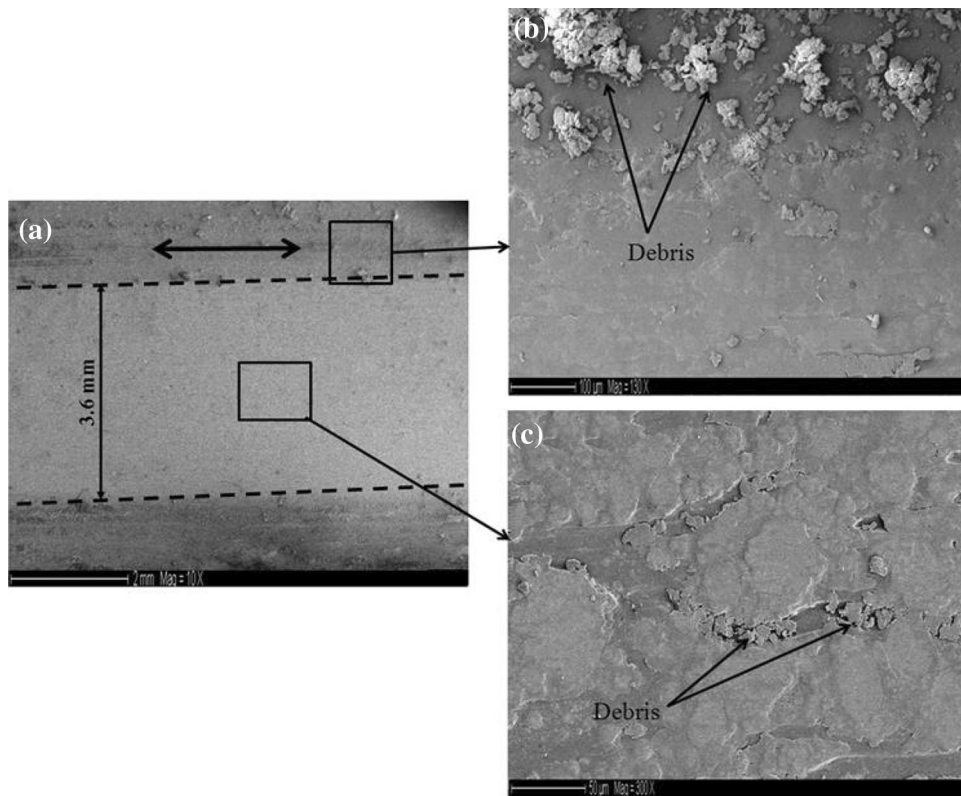


Fig. 15 Worn surface of composite A observed by SEM after 36,000 cycles: **a** wear track, **b** edge of the wear track, and **c** mid of wear track

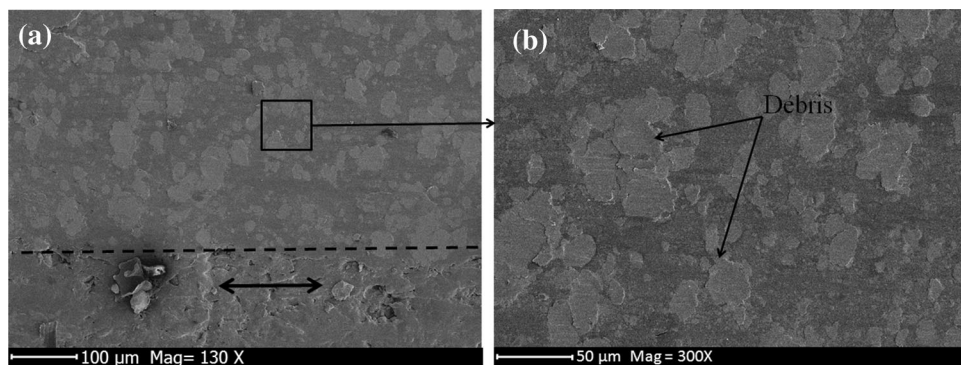


Fig. 16 Worn surface of composite C observed by SEM after 36,000 cycles: **a** wear track, and **b** mid of wear track

and can also be attributed to the presence of bronze particles. It is well known that a sufficient bronze content in the PTFE leads to a small scale lamellar structure and then the formation of small sized debris during sliding and its removal from the interface is difficult as illustrated by Fig. 15c. The existence of these debris in the interface for a long time protects the sample surface from both the transfer film as well as the third body debris. Composite C exhibits the lowest wear resistance. Thus, in the bulk material of the

composite C wt% of the bronze particles is less than that in composite A and B. Consequently, there is a large spacing of PTFE in contact with the steel counter face which activates the adhesion mechanism which leads to release of bronze particles. This is illustrated by the OM observation (Fig. 14b) and the SEM observation (Fig. 16b), respectively. Figure 20 shows that during sliding the debris is easily removed from the interface. The elimination of the debris from the interface accelerates the wear mechanism.

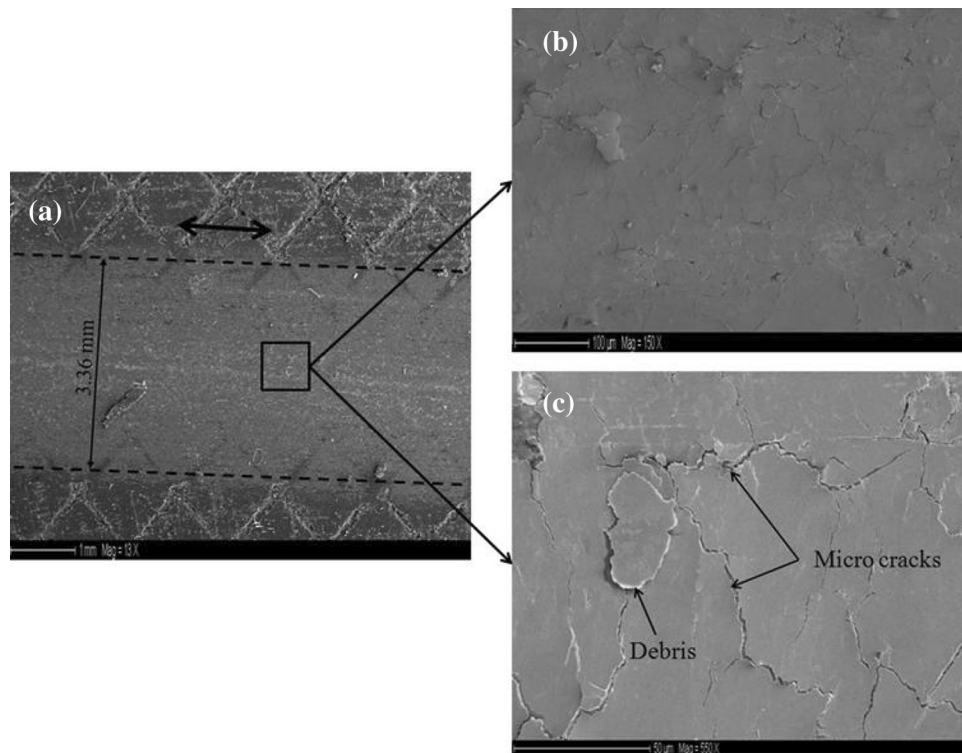


Fig. 17 Worn surface of composite B observed by SEM after 36,000 cycles: **a** wear track, **b** mid of wear track ($\times 150$) and **c** mid of wear track ($\times 550$)

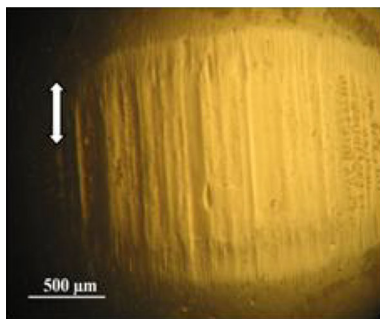


Fig. 18 Optical micrograph of the steel counterface rubbing for 36,000 cycles against composite B

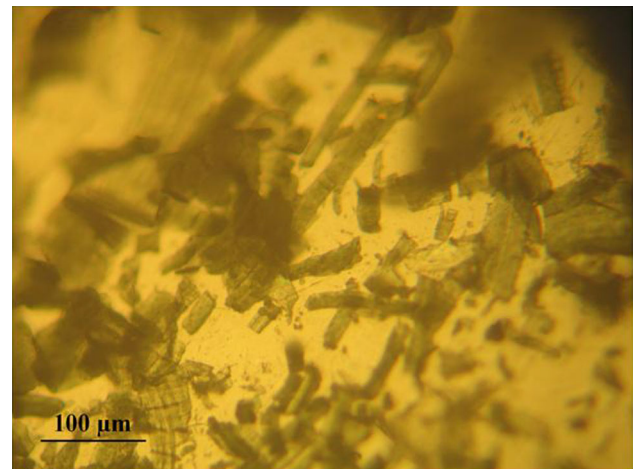


Fig. 19 Optical micrograph of the debris resulting from the sliding on the composite B

4 Conclusions

1. The ultimate strength of the PTFE composites decreases when it is filled with the MoS_2 . This is due to the low bond at the interface between the fillers and the PTFE.
2. The hardness tests showed, no significant difference between the PTFE composites, especially on addition of the MoS_2 .
3. Composite B has a good wear resistance but its friction behavior is not preferable. Thus, the incorporation of

the MoS_2 along with bronze contributes to decrease the specific wear rate of the composite by restraining the transfer of the PTFE to the steel counter face. But during the wear process, the composite interacts with the steel counter face under the effects of the thermal and shear stresses which leads to the formation of the



Fig. 20 Wear track of the composite C after 36,000 cycles

reaction products having an abrasive action on the steel counter face.

4. The lowest wear resistance of the PTFE bronze composite named “C” can be attributed to the low wt% of bronze.
5. The results show that PTFE bronze composite named “A” corresponds to the best friction and wear abilities.

References

1. Jisheng E, and Gawne D T, *Wear* **176** (1994) 195205.
2. Unal H, Sen U, and Mimaroglu A, *Mater Des* **27** (2006) 694699.
3. Sawyer W G, Freudenberg K D, Bhimaraj P, and Schadler L S, *Wear* **254** (2003) 573580.
4. Tevrüz T, *Wear* **230** (1999) 6169.
5. Khoddamzadeh A, Liu R, and Wu X, *Wear* **266** (2009) 646657.
6. Wang Y, and Yan F, *Wear* **262** (2007) 876882.
7. Tanaka K, and Kawakami S, *Wear* **79** (1982) 221234.
8. Bahadur S, and Tabor D, *Wear*, **98** (1984) 113.
9. Qian-qian S, and Xian-hua C, *Wear*, **260** (2006) 12431247.
10. Jaydeep K, Ioan N, and Efstathios I M, *Wear* **252** (2002) 361369.
11. Cheng X H, Xue Y J, and Xie C Y, *Wear* **253** (2002) 869877.
12. Sung N, and Suh N, *Wear* **53** (1979) 129141.
13. Li F, Hu K A, Li J L, and Zhao B Y, *Wear* **249** (2002) 877882.
14. Beckford S, Wang Y A, and Zou M, *Tribol Trans* **54** (2011) 849858.
15. Sole B M, and Ball A, *Tribol Int* **29** (1996) 457465.
16. Cho M H, and Bahadur S, *Wear* **258** (2005) 835845.
17. NFT 51-034 Plastiques: Détermination des caractéristiques en traction, AFNOR, French Norm AFNOR (1981).
18. ISO 868 Plastics and ebonite: Determination of indentation hardness by means of a durometer, ISO, Shore hardness (1985).
19. G 99-05 Standard Test Method for Wear Testing with a Pin-on-Disk Apparatus, ASTM International, USA (2005).
20. Lauer J L, Bunting B G, and Jones W R, *Tribol Trans* **31** (1988) 282288.
21. Gony D L, Zhang B, Xue Q J, and Wang H L, *Wear* **137** (1990) 267273.
22. Zhang H J, Zhang Z Z, and Guo F, *Tribol Trans* **54** (2011) 417423.
23. Xiubing L, Yimin G, Jiandong X, Yu W, and Liang F, *Wear* **257** (2004) 279283.
24. Li F, Yan F Y, Yu L G, and Liu W M, *Wear* **237** (2000) 3338.